Results in Chemistry 3 (2021) 100237

Contents lists available at ScienceDirect

Results in Chemistry

journal homepage: www.sciencedirect.com/journal/results-in-chemistry

Pyclen-based Gd complex with ionisable side-chain as a contrastophore for the design of hypersensitive MRI nanoprobes: Synthesis and relaxation studies

Fabienne Dioury [a,*], Maité Callewaert [b], Cyril Cadiou [b], Céline Henoumont [c], Michael Molinari [d], Sophie Laurent [c,e], Christophe Portefaix [f,g], Marc Port [a], Francoise Chuburu [b,*]

[a] Conservatoire national des arts et métiers, GBCM Laboratory, EA 7528, 2 rue Conté, 75003 Paris, HESAM Université, France
[b] Institut de Chimie Moléculaire de Reims, CNRS UMR 7312, University of Reims Champagne-Ardenne URCA, 51685 Reims Cedex 2, France
[c] NMR and Molecular Imaging Laboratory, University of Mons, UMons, B-7000 Mons, Belgium
[d] CBMN CNRS UMR 5248, University of Bordeaux, INP Bordeaux, 33600 Pessac, France
[e] Center for Microscopy and Molecular Imaging, Rue Adrienne Bolland 8, B-6041 Charleroi, Belgium
[f] Radiology Department, CHU de Reims – Hôpital Maison Blanche, 45 Rue Cognacq-Jay, 51092 Reims Cedex, France
[g] CReSTIC Laboratory, EA 3804, University of Reims Champagne-Ardenne URCA, 51685 Reims Cedex 2, France

ARTICLE INFO

Keywords:
PCTA chelating agent
Gadolinium contrast agent
Nanohydrogel

ABSTRACT

A straightforward method for synthesizing at the multigram scale a low molecular weight PCTA-based gadolinium complex bearing an ionizable oxyacetic chain on the pyridine unit was described, together with its encapsulation within a nanohydrogel matrix. The ionic gelation occurred between chitosan and hyaluronic acid, reinforced by crosslinking with sodium tripolyphosphate. The resulting nanogels are spherical and narrowly monodisperse. They are stable for at least four months at room temperature in water and in media of higher ionic strength (NaCl 0.9%, PBS). They display an enhanced longitudinal relaxivity r_1 of 15.9 and 12.1 $mM^{-1}.s^{-1}$ at 20 MHz and 60 MHz at 37 °C respectively which is at least 4 times higher than that of DOTAREM®.

Introduction

Over the years, magnetic resonance imaging (MRI) has become one of the key diagnostic tools in radiology due to its noninvasive nature and theoretically infinite penetration depth. Furthermore, this technique provides images with excellent anatomical resolution, in a real-time monitoring manner. To compensate the low sensitivity of the technique and to reinforce the image contrast, millimolar concentrations of paramagnetic contrast agents are often injected as contrastophores. To date, the commercially available paramagnetic systems are gadolinium-based contrast agents (GBCAs) [1] and are used in about 40% of all magnetic resonance imaging exams [2]. Usually administered at doses of 0.1 mmol per kg, GBCAs have the ability to shorten T_1 relaxation times of water protons in the tissues where they distribute and thus to highlight pathological areas. *In vitro*, the efficacy of GBCAs is measured in terms of relaxivity r_1 which is defined as the relaxation rate enhancement of the water proton per millimolar Gd(III) ion.

As free gadolinium Gd(III)) is toxic, in GBCAs it is usually chelated with high denticity ligands that encircles it while leaving free a coordination position for a water molecule [3]. During the last decades, many efforts have been made to develop such ligands able to ensure to GBCAs a good thermodynamic stability as well as a chemical inertia towards Gd dissociation [1], and two categories of ligands have been developed. They are polyaminocarboxylate ligands for which the skeleton is either linear or macrocyclic. For GBCAs that relied upon linear structures, the stability factors are lower than those for GBCAs based upon macrocyclic structures [4], and recently, the question of linear GBCAs safety has prompted the European Medicines Agency (EMA) to suspend the use of all linear GBCAs [5]. Therefore, the need for safer and more sensitive contrast agents remains essential to have effective and non-toxic GBCAs to detect pathological abnormalities under good conditions. Alternatives to current contrast agents are thus needed not only from the point of view of the nature of the ligand ensuring good thermodynamic stability and chemical inertia, but also from the point of

Abbreviations: PCTA, Pyridine-Containing triaza macrocycle TriAcetate; PBS, Phosphate Buffered Saline; DIPEA, N,N-Diisopropylethylamine (Hünig's base).

* Corresponding authors.
E-mail addresses: fabienne.dioury@lecnam.net (F. Dioury), francoise.chuburu@univ-reims.fr (F. Chuburu).

https://doi.org/10.1016/j.rechem.2021.100237
Received 23 July 2021; Accepted 2 November 2021
Available online 6 November 2021

view of its effectiveness in accelerating the relaxation of protons from water molecules (*i.e* improving the relaxivity r_1).

In this paper, both aspects were considered. To this end, the multigram scale synthesis of the low molecular weight ligand **LH_4** based on a PCTA (3,6,9,15-tetraazabicyclo[9.3.1] pentadeca-1(15),11,13-triene-3,6,9,-triacetic acid) scaffold (Scheme 1) was revisited. Indeed, PCTA is known to be a well-suited chelating agent for lanthanide ions, leading to stable chelates [6–9] with fast kinetics of complex formation and high kinetic inertness [10]. The PCTA scaffold was first modified by the addition of an oxyacetic chain on the pyridine unit and, in a second time, the corresponding **GdLH** chelates [11] were incorporated within nanohydrogels. The nanohydrogels under consideration were obtained by an ionic gelation process [12] between two hydrophilic biopolymers, namely chitosan (CS) which is polycationic, and hyaluronic acid (HA) which is polyanionic. Since the nanogel formation is driven by electrostatic interactions, it justifies the need to add an ionizable function on the PCTA scaffold to favor **GdLH** encapsulation. Finally, the ability of encapsulated **GdLH** chelates to better accelerate the proton relaxation rates of water molecules in their vicinity was evaluated by relaxometric experiments.

Results and discussion

*Syntheses of **LH_4** and its gadolinium complex **GdLH***

The synthesis of the desired gadolinium complex **GdLH** was performed with two post-macrocyclization steps from the prochelator **$LtBu_4$** (Scheme 1).

The strategy is based on a key macrocyclization step that involves the two pre-functionalized synthons **1** and **2** [13] so that all the functions required for both complexation of the paramagnetic ion and encapsulation in hydrogels are already installed on the resulting prochelator. This method, by assembling two "blocks", has the advantage of avoiding high-dilution and limiting the number of post-macrocyclization steps and is well-adapted to the synthesis of **$LtBu_4$** at the multigram scale. Indeed, this strategy proved to be more efficient in terms of overall yield than those based on regioselective functionalization after macrocyclization [14]. Moreover, the block assembly strategy is also well-suited to the preparation of custom-made pyclen-based chelating agents as structural variations can be done on both blocks. For instance, it allows to modulate the ligand denticity according to the metallic cation to be chelated and/or the nature of the additional site according to the desired application (bioconjugation, bimodal tracer, encapsulation, …) [13–19].

Compound **$LtBu_4$** resulted from a controlled macrocyclization step [14,15] involving the linear triamine **2** [13,18] and the dibromomethyl pyridine **1**. Triamine **2** was prepared from diethylenetriamine at scales up to 15 g with an overall yield of 60% following a three-step process recently reported by us [13]. Dibromide **1** was also prepared at scales up to 20 g in accordance to the previously described procedure for the ethyl ester analogue [13].

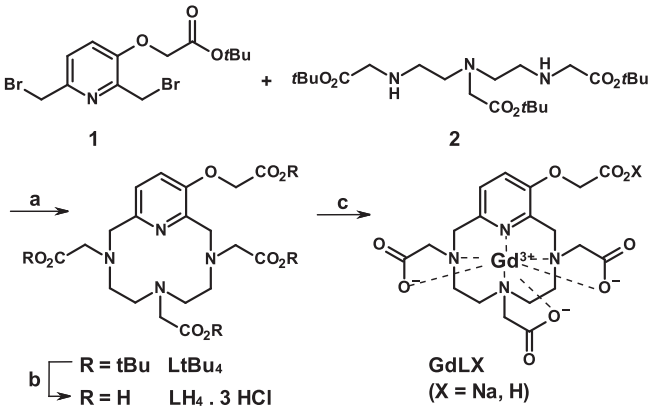

Scheme 1. Synthesis of the gadolinium complex mentioned in this work. a) Na_2CO_3, CH_3CN; b) HCl_{anh}, Et_2O; c) $GdCl_3$, H_2O, NaOH, H_2O, *pH* 5.5 then NaOH, *pH* 7.5.

The nucleophilic displacement of bromide for ring closure is not so trivial as it can give rise to several by-products: competitive [2 + 2] macrocyclic products together with oligomeric forms, competitive conversion of triamine synthon into non-reactive lactam [16]. Therefore, as Picard's group has done previously for bifunctional chelating agents bearing a *para*-substituent on the pyridine, or on one of the α-carbon of an acetate arm [17], we examined the macrocyclization conditions for scaling-up (Table 1).

Based on our previous results for the ethyl series compound [13], the conditions for the selective formation of the 12-membered ring compound **$LtBu_4$** resulting from a [1 + 1] macroring process were applied to the dibromide **1** of the tert-butyl series. This led to the compound **$LtBu_4$** obtained in 72% yield for a scale of more than 3 g (*Entry 1*). Interestingly, a similar result was obtained in homogeneous medium with *N,N*-diisopropylethylamine in dichloromethane which excludes the "metal-template" ion effect [20] as the dominant factor in this macrocycling process (*Entry 2*) [18]. However, from a practical point-of-view, the heterogeneous conditions were preferred because the treatment to remove the base from the crude is easier (simple filtration *versus* repeated washings of the organic solution). It is also interesting to note, based on ^{1}H NMR monitoring of the crudes, that the 5-fold increase of the reaction concentration had little or no impact on the [1+1]-macroring process with a satisfactory yield of about 70–75% and a similar purity for the isolated 12-membered macrocycle **$LtBu_4$** (*Entry 3*; *see ESI for details*). However, for the higher concentration of 0.22 *M*, the yield dropped to 50% and was accompanied by a significant loss of purity of the isolated product. This can be attributed, on the basis of the ^{1}H NMR spectrum showing broad resonances superimposed on those of the 12-membered macrocycle **$LtBu_4$**, to competitive side-processes of oligomerization and/or [2 + 2]-macroring (*Entry 4*; *see ESI*).

As reported for other PCTA compounds [13,17,18], the compound **$LtBu_4$** is characterized by a specific ^{1}H NMR feature that can be attributed to its intrinsic overall basicity. Indeed, considering the calculated pK_a*s* and the corresponding distribution curves of the species in solution, the strongest basic center would be nitrogen *N6* opposite to the pyridine subunit with a *pKa* value of 6 (*see ESI*) [21]. Therefore, at pH 5–6, reached when the alkaline crudes are washed to neutrality, the compound **$LtBu_4$** may exist as a mixture of acidic + 1-charged species in equilibrium on the NMR timescale, and can explain the ^{1}H NMR trace obtained with strong line-broadening for all the CH_2 resonances in the 2.5–5.0 ppm region. On the opposite, samples resulting from a basic medium *pH* greater than 8 exhibit a ^{1}H NMR spectrum with sharp signals and the methylenic protons in the 3.0–4.2 ppm region split into AB patterns (*see ESI*). This may be consistent with the occurrence of a single species, corresponding to an uncharged species or to a Na-complex as reported before for similar compounds [17]. Furthermore, similar *pH*-dependence can be observed as well on ^{13}C NMR traces (*see ESI*).

Table 1
Optimization of the macrocyclization conditions for compound **$LtBu_4$**. Experimental conditions: a solution of triamine **2** in acetonitrile or dichloromethane at the indicated concentration (0.01 to 0.22 *M*), with dibromide **1** (1.1 eq) and a base (Na_2CO_3 or DIPEA) was stirred at room temperature overnight.

Entry	Solvent	Triamine **2** (mol. L^{-1})	Base (eq)	Yield (mass obtained)
1[a)]	CH_3CN	0.01	Na_2CO_3 (4 eq)	72% (3.4 g)
2	CH_2Cl_2	0.01	DIPEA (3 eq)	71% (1.1 g)
3	CH_3CN	0.05	Na_2CO_3 (4 eq)	76% (1.2 g)
4	CH_3CN	0.22	Na_2CO_3 (4 eq)	51% (0.8 g)

(a) Conditions previously reported for analogous pyclen-based prochelator [13].

The deprotection of the *tert*-butyl esters was then achieved by acidolysis in anhydrous hydrogen chloride at room temperature and afforded the tetraacid **LH_4** in the form of a hydrated trihydrochloride salt **LH_4. 3HCl·2H_2O** with a yield of 65% after purification by reverse phase chromatography. In order to examine the acid-base properties of the compound **LH_4**, a ^{1}H NMR titration was then performed according to the protocol described by S. Aime *et al.* [6]. In addition, as done by G. Tircsó *et al.* [10], the titration was performed over a wide range of pH 1–13 in order to determine as many pK_as values as possible within this range (*See ESI for details*). Under these conditions, six protonation steps were detected (pK_as ≈ 2.0, 2.5, 4.0, 7.0, 8.1, 10.4) so that it can be assumed that the *meta* substituent induces an increase in total basicity since three protonations occured in the *pH*-range 6–13 whereas two ones were reported in the same range for the parent ligand PCTA-12 [6,7,10,22].

Finally, the Gd-complexation proceeded rapidly in less than 2.5 h with a stoichiometric amount of $GdCl_3$ at 50–55 °C and at a controlled *pH* of 5.5 and gave the complex **GdLH** in 82% yield after removal of free Gd^{3+} by precipitation as its hydroxide salt (*pH* raised to 7.5 with NaOH) followed by a desalting procedure by membrane filtration and gel filtration on Sephadex™ G-10. Luminescence lifetime measurements performed in H_2O and D_2O (*see ESI*) on the corresponding Eu(III) complex allowed to determine that two water molecules were directly coordinated to the lanthanide ion [23].

Encapsulation of GdLH within nanogels

GdLH ⊂ CS-TPP/HA nanogels (NGs) were prepared by a one-step ionotropic gelation process [12]. This method relied upon the establishment of multivalent electrostatic interactions between chitosan (CS) and hyaluronic acid (HA). The resulting supramolecular network could be reinforced by cross-linking mediated by small anionic cross-linkers such as sodium tripolyphosphate (TPP). The average hydrodynamic diameters of **GdLH** ⊂ CS-TPP/HA NGs were determined by DLS as well as the polydispersity index of the nanoparticle population (Table 2). Nanoparticle zeta potential (ζ) which was indicative of their outermost surface charge was determined by ELS.

DLS analysis showed that before dialysis **GdLH** ⊂ CS-TPP/HA nanogels exhibited average hydrodynamic diameters inferior to 300 nm. Upon dialysis, one should notice that the NG size increased which can be attributed to the NG swelling and the hydrogel nature of the nano-objects [24]. DLS monitoring of nanogel sizes over a period of four months demonstrated that owing to electrostatic repulsion (ξ-potential >+38 mV after dialysis), the final colloidal suspensions were stable at room temperature (Fig. 1). In higher ionic strength media such as NaCl 0.9% or PBS, the initial NG hydrodynamic diameter is lowered due to the shrinking of the double ionic layer that surrounds the nanoparticles [25]. Moreover, no modification of the hydrodynamic diameter was observed over a long period of time illustrating the long-term stability of these NGs in these physiological media.

Scanning Electron Microscopy (SEM) analysis (Fig. 2*a*) highlighted that **GdLH** ⊂ CS-TPP/HA nanogels were spherical and narrowly monodisperse. The diameters determined by SEM were in the range of 120–170 nm and then, smaller compared to the DLS ones. This is usually observed because of the dehydration occurring during sample drying. The presence of Gd(III) inside the NGs was confirmed by energy-dispersive X-ray spectroscopy (EDXS) performed on isolated

Table 2
Nanogel characteristics and Gd(III) loadings of **GdLH** ⊂ CS-TPP/HA NGs.

D_H (nm) before dialysis [a)]	254
D_H (nm) after dialysis [a)]	281
PdI	0.15
ξ (mV)	38
$[Gd]_{NGs}$ (mM)	0.12

(a) Measure in intensity.

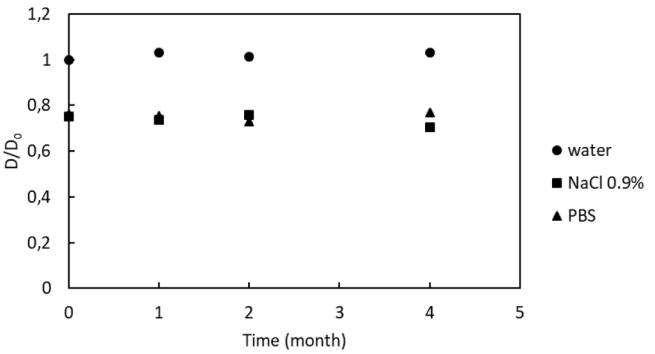

Fig. 1. Particle size variation as a function of time (D refers to the diameter at time t and D_0 to the initial diameter).

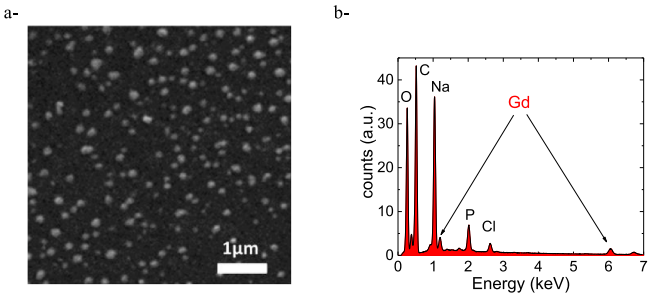

Fig. 2. a- SEM images of **GdLH** ⊂ CS-TPP/HA NGs; b- EDXS spectrum of **GdLH** ⊂ CS-TPP/HA NGs showing a characteristic Gd signal.

nanoparticles (Fig. 2*b*). On the EDXS spectrum, in addition to the current elements constituting of the nanogel, the characteristic lines of Gd were clearly observed. Gd loadings determined by ICP–OES measurements were comparable to those already obtained for GdDOTA ⊂ CS–TPP/HA nanogels [26], depicting the versatility of the encapsulation process.

MRI efficiency of **GdLH** ⊂ CS-TPP/HA nanogels was evaluated by means of their longitudinal relaxation rates and their NMRD profile was recorded at 37 °C (*see ESI*).

On a per millimolar-Gd basis, the **GdLH** ⊂ CS-TPP/HA nanosuspension presented a r_1 value of 15.9 $mM^{-1}.s^{-1}$ at 20 MHz and 12.1 $mM^{-1}.s^{-1}$ at 60 MHz (*see ESI*). In comparison, the free complex **GdLH** for which the gadolinium center possesses two coordinated water molecules, was characterized by a r_1 of 7.4 $mM^{-1}.s^{-1}$ at 20 MHz and 6.7 $mM^{-1}.s^{-1}$ at 60 MHz [13]. The particles exhibited then a relaxivity exaltation (*i.e.* almost 2 times higher at 20 and 60 MHz respectively) and compared to the gold standard DOTAREM®, an exaltation of relaxivity of at least a factor of 4 in the same frequency range. Moreover, the **GdLH** ⊂ CS-TPP/HA NGs NMRD profile was characterized by a maximum in relaxivity between 25 and 30 MHz which is typical for Gd complexes with a restricted rotational motion (*see ESI*). This restriction is due to the encapsulation of GBCAs within the nanogels [12]. Furthermore, as both CS and HA are highly hydrophilic [27], they provide a favorable aqueous environment for **GdLH** chelates via H-bonding interactions between water molecules and Gd chelates. Thus, the polymeric hydrophilic matrix has a positive impact on Gd chelate relaxivity since for Gd chelates burried within this matrix, it was enhanced probably *via* an outer-sphere and/or second-sphere mechanisms [26]. In order to check how this relaxation amplification could be translated into high-field MR images as well, T_1-weighted images of phantoms containing **GdLH** ⊂ CS–TPP/HA suspensions were acquired on a 3 T clinical imager, with DOTAREM® as control (Fig. 3). The T_1–weighted images revealed that the signal brightening as a function of Gd concentration is much higher when **GdLH** is encapsulated in nanogels. There are two physical reasons for this: encapsulation of large

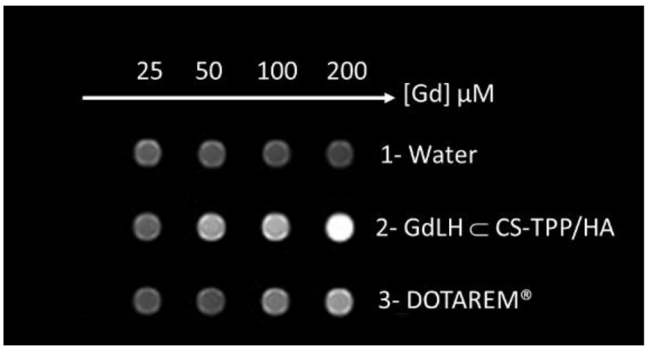

Fig. 3. T_1- weighted images of **GdLH** ⊂ CS-TPP/HA NGs (line 2), DOTAREM® (line 3) and water (line 1) as controls. All samples were imaged at 3 T (128 MHz).

amounts of **GdLH** in nanogels led first in an apparent increase in the mass of the complex and second in a restriction of its rotational motion. These two effects led to a great exaltation of the MRI signal [28].

Conclusion

The PCTA-based gadolinium chelate **GdLH** was synthesized at the multigram scale. The strategy is based on the assembly of two functionalized blocks to build the macrocyclic scaffold followed by two post-macrocyclization steps and led to the desired chelate with an overall yield for three steps of 40%. **GdLH** encapsulation within nanogel through an ionic gelation process resulted in a boost in relaxation by at least a factor of 4 (in the range 20–60 MHz), by comparison to the gold standard DOTAREM®. The incorporation of gadolinium chelates in highly hydrophilic matrices such as nanohydrogels is therefore a simple way to substantially amplify the MRI response of gadolinium chelates without the need for sophisticated synthetic strategies. These results encouraged us to plan further investigations with variation either on the nature of the ionisable side-chain (cationic, zwitterionic) or on the nanogel matrix in order to have **GdLH** nanogels that can be addressed to specific targets.

CRediT authorship contribution statement

Fabienne Dioury: Methodology, Validation, Investigation, Writing–original draft, Writing – review & editing. **Maité Callewaert:** Methodology, Validation, Investigation, Funding acquisition. **Cyril Cadiou:** Methodology, Validation, Investigation. **Céline Henoumont:** Methodology, Validation, Investigation, Writing – review & editing. **Michael Molinari:** Methodology, Validation, Investigation. **Sophie Laurent:** Resources, Supervision, Funding acquisition, Writing – review & editing. **Christophe Portefaix:** Methodology, Validation, Investigation. **Marc Port:** Supervision, Writing – review & editing. **Francoise Chuburu:** Conceptualization, Supervision, Writing–original draft, Writing – review & editing.

Declaration of Competing Interest

The authors declare that they have no known competing financial interests or personal relationships that could have appeared to influence the work reported in this paper.

Acknowledgements

The authors would like to thank the “Programme de coopération transfrontalière Interreg France-Wallonie-Vlaanderen” for funding the “Nanocardio” project (http://nanocardio.eu), the PHC Brancusi program (project n° 43465WA), and the PlAneT platform (supported by the European Regional Development Fund and the Region Champagne-Ardenne). The authors thank the NanoMat platform supported by the European Regional Development Fund, the DRRT Grand Est and the Region Grand Est and especially Dr N.B. Bercu for his technical assistance. This work was also performed with the financial support of the FNRS, FEDER, the ARC, the Walloon Region (Biowin and Interreg projects) and the COST actions. Authors thank the Center for Microscopy and Molecular Imaging (CMMI, supported by European Regional Development Fund Wallonia) and the Bioprofiling platform (supported by the European Regional Development Fund and the Walloon Region, Belgium).

Appendix A. Supplementary data

Supplementary data to this article can be found online at https://doi.org/10.1016/j.rechem.2021.100237.

References

[1] M. Port, J.-M. Idée, C. Medina, C. Robic, M. Sabatou, C. Corot, Efficiency, thermodynamic and kinetic stability of marketed gadolinium chelates and their possible clinical consequences: a critical review, Biometals 21 (4) (2008) 469–490, https://doi.org/10.1007/s10534-008-9135-x.
[2] J. Wahsner, E.M. Gale, A. Rodríguez-Rodríguez, P. Caravan, Chemistry of MRI contrast agents: current challenges and new frontiers, Chem. Rev. 119 (2) (2019) 957–1057, https://doi.org/10.1021/acs.chemrev.8b00363.
[3] T.J. Clough, L. Jiang, K.-L. Wong, N.J. Long, Ligand design strategies to increase stability of gadolinium-based magnetic resonance imaging contrast agents, Nat. Commun. 10 (1) (2019) 1420, https://doi.org/10.1038/s41467-019-09342-3.
[4] T.J. Fraum, D.R. Ludwig, M.R. Bashir, K.J. Fowler, Gadolinium-based contrast agents: a comprehensive risk assessment, J. Magn. Reson. Imaging 46 (2) (2017) 338–353, https://doi.org/10.1002/jmri.v46.210.1002/jmri.25625.
[5] European Medecines Agency. Gadolinium-Containing Contrast Agents. *https://www.ema.europa.eu/en/medicines/human/referrals/gadolinium-containing-contrast-agents*. 2017.
[6] S. Aime, M. Botta, S. Geninatti Crich, G.B. Giovenzana, G. Jommi, R. Pagliarin, M. Sisti, Synthesis and NMR studies of three pyridine-containing triaza macrocyclic triacetate ligands and their complexes with lanthanide ions, Inorg. Chem. 36 (14) (1997) 2992–3000, https://doi.org/10.1021/ic960794b.
[7] J.-M. Siaugue, A. Favre-Réguillon, F. Dioury, G. Plancque, J. Foos, C. Madic, C. Moulin, A. Guy, Effect of mixed pendant groups on the solution properties of 12-membered azapyridinomacrocycles: evaluation of the protonation constants and the stability constants of the europium(III) complexes, Eur. J. Inorg. Chem. 2003 (15) (2003) 2834–2838, https://doi.org/10.1002/ejic.200300016.
[8] M. Port, I. Raynal, L. Vander Elst, R.N. Muller, F. Dioury, C. Ferroud, A. Guy, Impact of rigidification on relaxometric properties of a tricyclic tetraazatriacetic gadolinium chelate, Contrast Media Mol. Imaging 1 (3) (2006) 121–127, https://doi.org/10.1002/(ISSN)1555-431710.1002/cmmi.v1:310.1002/cmmi.99.
[9] S. Aime, M. Botta, S.G. Crich, G.B. Giovenzana, G. Jommi, R. Pagliarin, M. Sisti, MRI contrast agents: macrocyclic Lanthanide(III) complexes with improved relaxation efficiency, J. Chem. Soc., Chem. Commun. 18 (1995) 1885–1886, https://doi.org/10.1039/C39950001885.
[10] G. Tircsó, Z. Kovács, A.D. Sherry, Equilibrium and formation/dissociation kinetics of some LnIIIPCTA complexes, Inorg. Chem. 45 (23) (2006) 9269–9280, https://doi.org/10.1021/ic060875010.1021/ic0608750.s001.
[11] M. Port, Lipophilic Chelates and Use Thereof in Imaging. WO2006100305, March 24, 2006.
[12] T. Courant, V.G. Roullin, C. Cadiou, M. Callewaert, M.C. Andry, C. Portefaix, C. Hoeffel, M.C. de Goltstein, M. Port, S. Laurent, L.V. Elst, R. Muller, M. Molinari, F. Chuburu, Hydrogels incorporating GdDOTA: towards highly efficient dual T1/T2 MRI contrast agents, Angew. Chem. Int. Ed. 51 (36) (2012) 9119–9122, https://doi.org/10.1002/anie.201203190.
[13] M. Devreux, C. Henoumont, F. Dioury, D. Stanicki, S. Boutry, L. Larbanoix, C. Ferroud, R.N. Muller, S. Laurent, Bimodal probe for magnetic resonance imaging and photoacoustic imaging based on a PCTA-derived gadolinium(III) complex and ZW800-1, Eur. J. Inorg. Chem. 2019 (29) (2019) 3354–3365, https://doi.org/10.1002/ejic.201900387.
[14] F. Dioury, S. Sambou, E. Guéné, M. Sabatou, C. Ferroud, A. Guy, M. Port, Synthesis of a tricyclic tetraazatriacetic ligand for gadolinium(III) as potential contrast agent for MRI, Tetrahedron 63 (1) (2007) 204–214, https://doi.org/10.1016/j.tet.2006.10.024.
[15] J. Yong-Sang, F. Dioury, V. Meneyrol, I. Ait-Arsa, J.-P. Idoumbin, F. Guibbal, J. Patché, F. Gimié, I. Khantalin, J. Couprie, P. Giraud, S. Benard, C. Ferroud, E. Jestin, O. Meilhac, Development, synthesis, and 68Ga-labeling of a lipophilic complexing agent for atherosclerosis PET imaging, Eur. J. Med. Chem. 176 (2019) 129–134, https://doi.org/10.1016/j.ejmech.2019.05.002.
[16] C. Ferroud, H. Borderies, E. Lasri, A. Guy, M. Port, Synthesis of a novel amphiphilic GdPCTA-[12] derivative as a potential micellar MRI contrast agent, Tetrahedron Lett. 49 (41) (2008) 5972–5975, https://doi.org/10.1016/j.tetlet.2008.07.160.

[17] N. Leygue, M. Enel, A. Diallo, B. Mestre-Voegtlé, C. Galaup, C. Picard, Efficient synthesis of a family of bifunctional chelators based on the PCTA[12] macrocycle suitable for bioconjugation, Eur. J. Org. Chem. 2019 (18) (2019) 2899–2913, https://doi.org/10.1002/ejoc.201900280.
[18] M. Enel, N. Leygue, N. Saffon, C. Galaup, C. Picard, Facile access to the 12-membered macrocyclic ligand PCTA and its derivatives with carboxylate, amide, and phosphinate ligating functionalities, Eur. J. Org. Chem. 2018 (15) (2018) 1765–1773, https://doi.org/10.1002/ejoc.201800066.
[19] G. Bort, S. Catoen, H. Borderies, A. Kebsi, S. Ballet, G. Louin, M. Port, C. Ferroud, Gadolinium-based contrast agents targeted to amyloid aggregates for the early diagnosis of Alzheimer's disease by MRI, Eur. J. Med. Chem. 87 (2014) 843–861, https://doi.org/10.1016/j.ejmech.2014.10.016.
[20] J.E. Richman, T.J. Atkins, Nitrogen analogs of crown ethers, J. Am. Chem. Soc. 96 (7) (1974) 2268–2270, https://doi.org/10.1021/ja00814a056.
[21] Chemicalize software was used for pKas calculations. *Developed by ChemAxon; Https://Chemicalize.Com/; April-May*; 2020.
[22] R. Delgado, S. Quintino, M. Teixeira, A. Zhang, Metal complexes of a 12-membered tetraaza macrocycle containing pyridine and N-carboxymethyl groups, J. Chem. Soc., Dalton Trans. 1 (1997) 55–64, https://doi.org/10.1039/A602311H.
[23] Beeby, A.; M. Clarkson, I.; S. Dickins, R.; Faulkner, S.; Parker, D.; Royle, L.; S. de Sousa, A.; A. Gareth Williams, J.; Woods, M. Non-Radiative Deactivation of the Excited States of Europium, Terbium and Ytterbium Complexes by Proximate Energy-Matched OH, NH and CH Oscillators: An Improved Luminescence Method for Establishing Solution Hydration States. *J. Chem. Soc., Perkin Trans. 2* **1999**, No. 3, 493–504. https://doi.org/10.1039/A808692C.
[24] N.A. Peppas, J.Z. Hilt, A. Khademhosseini, R. Langer, Hydrogels in biology and medicine: from molecular principles to bionanotechnology, Adv. Mater. 18 (11) (2006) 1345–1360, https://doi.org/10.1002/(ISSN)1521-409510.1002/adma.v18:1110.1002/adma.200501612.
[25] H. Jonassen, A.-L. Kjøniksen, M. Hiorth, Effects of ionic strength on the size and compactness of chitosan nanoparticles, Colloid Polym. Sci. 290 (10) (2012) 919–929, https://doi.org/10.1007/s00396-012-2604-3.
[26] M. Callewaert, V.G. Roullin, C. Cadiou, E. Millart, L. Van Gulik, M.C. Andry, C. Portefaix, C. Hoeffel, S. Laurent, L.V. Elst, R. Muller, M. Molinari, F. Chuburu, Tuning the composition of biocompatible Gd nanohydrogels to achieve hypersensitive dual T1/T2 MRI contrast agents, J. Mater. Chem. B 2 (37) (2014) 6397–6405, https://doi.org/10.1039/C4TB00783B.
[27] R. Dong, Y. Pang, Y. Su, X. Zhu, Supramolecular hydrogels: synthesis, properties and their biomedical applications, Biomater. Sci. 3 (7) (2015) 937–954, https://doi.org/10.1039/C4BM00448E.
[28] A. Gupta, P. Caravan, W.S. Price, C. Platas-Iglesias, E.M. Gale, Applications for transition-metal chemistry in contrast-enhanced magnetic resonance imaging, Inorg. Chem. 59 (10) (2020) 6648–6678, https://doi.org/10.1021/acs.inorgchem.0c00510.